FIRST COMPUTATION OF PARASITIC FIELDS IN LHC DIPOLE MAGNET INTERCONNECTS

A. Devred, CEA/Saclay, Gif-sur-Yvette, France and CERN, Geneva, Switzerland
B. Auchmann, Y. Boncompagni, V. Ferapontov, J.P. Koutchouk,
S. Russenschuck, T. Sahner, C. Vollinger, CERN

Abstract

The Large Hadron Collider (LHC), now under construction at CERN, will rely on about 1600 main superconducting dipole and quadrupole magnets and over 7400 superconducting corrector magnets distributed around the eight sectors of the machine. Each magnet type is powered by dedicated superconducting busbars running along the sectors and mounted on the iron yokes of the main dipole and quadruple magnets. In the numerous magnet interconnects, the busbars are not magnetically shielded from the beam pipes and produce parasitic fields that can affect beam optics. We review the 3-D models that have been developed with ROXIE to compute the parasitic fields and we discuss their potential impacts on machine performance.

INTRODUCTION

The LHC, presently being installed in the LEP tunnel at CERN, requires 1232 14.3-m-long, 2-in-1 aperture dipole magnets, 392 2-in-1 aperture quadrupole magnets and a large number of single-aperture corrector magnets, which are superconducting and distributed in regular cells over 8 sectors [1]. The two counter-rotating proton beams cross at four interaction points and go alternately in the internal and external aperture of the main magnets as they circulate around the various sectors. Extensive analyses have been carried out to assess the field quality of individual magnets. However, no estimate was made so far of the field perturbations generated by the busbars in the magnet interconnects, which run in the beam pipes' proximity without being magnetically shielded by an iron yoke as in the magnet cold masses. This paper describes a 3-D ROXIE model of main busbars that was developed to compute the field perturbations generated in a typical, ~1.25-m-long, arc dipole-to-dipole magnet interconnect and to assess their influence on selected beam parameters.

In addition to the main busbars, a connection line of 2x21 (or 2x24, depending on the position) sc wires, the so-called *N*-line, and a 2x3-wire cable that is used for the powering of the dispersion suppressor magnets run along some interconnects. These two lines mix pairs of power and return wires and are heavily twisted (with a twist pitch ranging from 7.5 to 14 cm for the *N*-line and of 12 cm for the 2x3-wire cable). As a result, the fields produced by these wires are expected to be small with respect to those generated by the main busbars, leading us to concentrate on the latter. In this first pass, we also do not consider the contributions of the so-called connection cryostats and of the Distribution Feed Boxes (DFB).

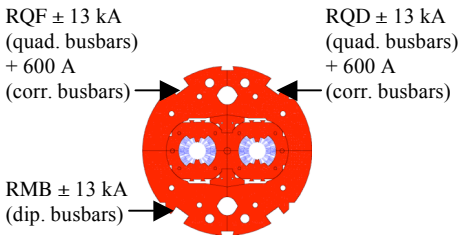

Figure. 1: Main busbars and current polarities in LHC arcs (viewed from dipole magnet connection side).

INTERCONNECT TOPOLOGY

In each sector, the magnets of a given type are connected electrically in series by pairs of superconducting busbars. In total, there are 6 active pairs (see Fig. 1): 1 for the main dipoles, 2 for the 2 apertures of the main quadrupoles and 3 for the corrector magnets (plus 2 spares). Here, we consider all busbars powered at their maximum current (13 kA for the dipole and quadrupole busbars and 600 A for the corrector busbars). The main busbar currents change polarity after each interaction point when the beams change aperture, but the corrector busbars do not. As the positioning of the dipole busbars is not symmetric with respect to the two apertures, we must consider 4 configurations, depending on which beam is in which aperture and on the main busbars' polarity. There are ~205 interconnects per sector, and, in average over a turn, each beam goes half of the time in the internal aperture and the other half in the external aperture.

ANALYTICAL ESTIMATE

The magnetic field in a given aperture is expressed as

$$B_y^{i,e}(x,y) + iB_x^{i,e}(x,y) = \sum_{n=1}^{\infty} (B_n^{i,e} + iA_n^{i,e}) \left(\frac{x+iy}{R_{ref}} \right)^{n-1} \qquad (1)$$

where x and y are the transverse coordinates, R_{ref} is the reference radius (17 mm for LHC), and B_n and A_n are the normal and skew $2n$-pole field components (in T). The i and e superscripts refer to the internal and external apertures.

As a first step, analytical estimations of the combined effects of the three pairs of main busbars powered with 13 kA have been carried out. The computation assumes that the busbars are straight and neglects the expansion loops visible in Fig. 2. The busbars are described as single line currents located at the barycentre of their cross-sections. The results are given in Table 1.

Table 1. Analytical estimates of multipole field perturbations produced by main busbars powered with 13 kA (for beam 1 in internal aperture; mT).

	ΔA_n		ΔB_n	
n	Internal	External	Internal	External
1	-2.30	-0.72	2.25	5.67
2	0.57	0.00	0.76	-1.39
3	0.16	-0.05	-0.45	-0.10

NUMERICAL CALCULATION

The CERN ROXIE code relies on the coupling of boundary-element (BEM) and finite-element (FEM) methods to compute electromagnetic fields in domains including conductors, non-linear magnetic materials and a surrounding air region [2]. For LHC magnets, the iron yokes are modelled by FEM meshes and the superconducting coils and busbars are in the BEM domain. Every cable strand is represented as a line-current, which, in 3-D, is split into a chain of segments following the cable trajectory. (Note that the Rutherford-type cable twist is not taken into account). The field contribution of each segment is calculated from Biot and Savart's law and partakes to the BEM source term. The solution for the entire problem domain is found by solving the fixed-point problem of coupled BEM and FEM equations.

Modelling

In ROXIE, the yoke geometry is created in 2-D and is extruded into the third dimension. Similarly, the coil design starts with a layout of the 2-D cross-section and proceeds to build 3-D shapes of the cables in the ends. As for the busbars, there are no parameterized options and the actual conductors' shape needs to be retrieved from technical drawings and put into ROXIE by means of brick elements. Bricks are pieces of cable defined by 2 oriented cross-sections, a number of layers, N_1, a number of strands per layer, N_2, and a total current, I, flowing from cross-section 1 to 2 in the (N_1xN_2) strands. A cross-section is defined by its 4 corner points and its orientation is provided by the ordering of these points. A busbar model comprises up to several hundreds of oriented cross-sections.

Given the complexity of the busbars' trajectories, it was decided to devise an automated way of extracting information from electronic drawings. The LHC interconnect drawings were produced with EUCLID, but, the busbar drawings were not all created in the same way. Some were depicted by mere lines, while others were represented by bricks or extruded from 2-D shapes and all of them lacked the current direction. The method finally adopted consisted in creating new and simplified EUCLID models. The new models contained only one guiding line, representing one edge of a busbar, and a number of closed lines at various vertexes along the guiding line representing busbar cross-sections. Each busbar was redrawn in EUCLID and a EUCLID-to-ROXIE routine was written to retrieve the busbar models and cross-section information from the drawing database.

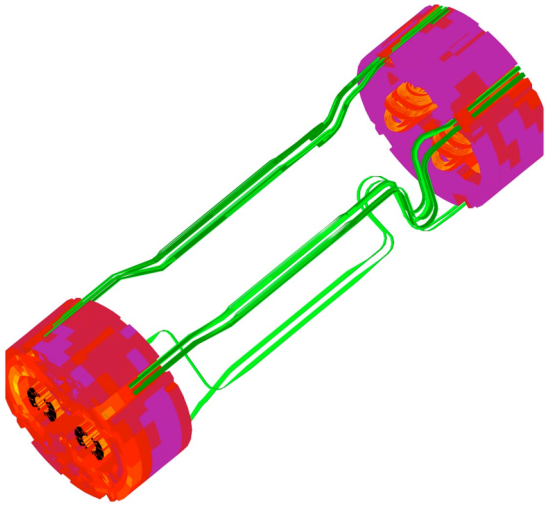

Figure 2: ROXIE model of an arc dipole-to-dipole busbar interconnect with coils ends and surrounding iron yoke.

At this stage, another problem arose. The strands are represented by line-current segments, joined at certain angles to mimic the busbars' trajectories. However, sharp angles in line currents produce field singularities. To smoothen the singularities and compute more realistic field values, the output of the EUCLID-to-ROXIE program was post-processed through an interpolation routine, which generated additional cross-sections.

Results

Fig. 2 shows the final ROXIE model of an arc dipole-to-dipole interconnect, featuring the coil ends (orange), the iron yoke (purple) and the busbars (green). It is one of the most elaborated models ever built with ROXIE and counts 58080 line-current segments for the coils, 41873 elements for the busbars and 1500 elements for the yoke.

To accurately estimate the iron yoke influence, it has to be in the saturated state where it is when the coils are fully energized. However, the coils' ends produce fringe fields that are orders of magnitude higher than those of the busbars and that are already included in the dipole field map. Hence, we started by computing the multipole fields of the complete geometry with busbars and coils powered, then, we computed the multipole fields produced by switching off the busbars, and, finally, we subtracted the latter from the former to derive the busbar perturbations. The results are illustrated in Fig. 3, while integrated values over the interconnect length (1224.4 mm) are reported in Table 2. In comparison to Table 1, it appears that the 3-D modelling cannot be avoided.

Table 2. ROXIE estimates of integrated multipole field perturbations produced by main and corrector busbars at full excitation (±13 kA and 600 A; mTxm).

	Beam 1				Beam 2			
	Internal		External		Internal		External	
n	ΔA_n	ΔB_n	ΔA_n	ΔB_n	ΔA_n	ΔB_n	ΔA_n	ΔB_n
1	1.59	1.63	0.55	12.8	2.74	1.34	-1.58	-9.35
2	0.27	1.72	-0.61	-2.46	-0.63	-1.27	0.28	2.18
3	-0.02	0.15	-0.27	0.75	-0.03	-0.16	0.29	-0.76

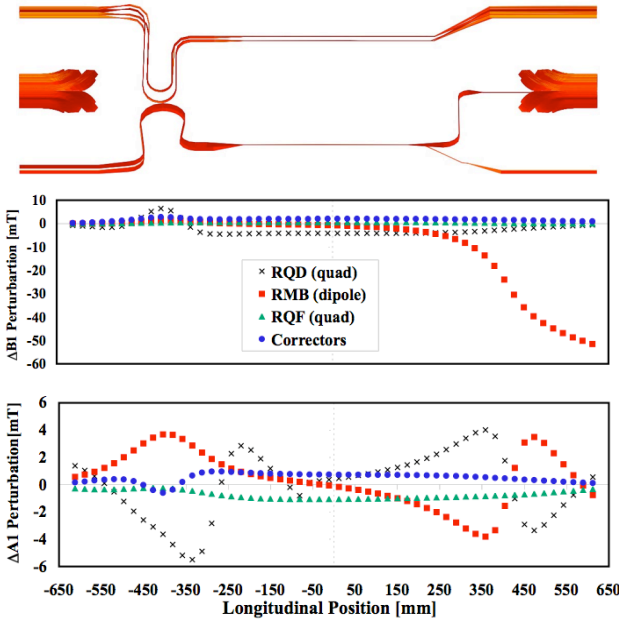

Figure 3. ROXIE computation of field perturbations generated by busbars (at full excitation and for beam 2 in external aperture): (a) ΔB_1 (top), (b) ΔA_1 (bottom).

Table 3: Estimated perturbations caused by fully-powered busbars on selected LHC beam parameters.

$\Delta\hat{x}_{\rm int}$ [μm]	59
$\lvert\Delta\mu_{\rm sec}\rvert$	0.008
$\lvert\Delta Q\rvert$	0.012
$\lvert c_{\rm sec}\rvert$	0.0040

EFFECTS ON BEAM OPTICS

The integrated field perturbations are at the level of a few mT×m, *i.e.*, a few units (10^{-4}) of the main field integral. Hence, we can use approximate equations for a first estimate of the perturbations to the beam optics. (Here, we rely on multipole fields derived from ROXIE.)

Closed Orbit Deviation

The amplitude of the horizontal closed orbit deviation, $\Delta\hat{x}_{\rm int}^{\rm i,e}$, caused on the internal (or external) aperture beam by the dipole field perturbation, $\Delta B_1^{\rm i,e}$, integrated over a single interconnect length and computed at the maximum of the beta function in the arc, is

$$\Delta\hat{x}_{\rm int}^{\rm i,e} \approx \frac{\beta_{\rm QF}}{2\sin(\pi Q_{\rm x})} \frac{\int_{\rm int} {\rm d}\sigma\, \Delta B_1^{\rm i,e}(\sigma)}{B\rho} \qquad (2)$$

where $\beta_{\rm QF}$ is the maximum beta function value (177), $Q_{\rm x}$ is the horizontal tune (64.31 at collision) and $(B\rho)$ is the magnetic rigidity ($23.357\text{x}10^3$ Txm at collision). A similar expression can be derived for the vertical deviation giving a slightly smaller orbit perturbation.

Table 3 shows that the perturbation caused by a single interconnect yields at most a 60-µm oscillation. As there is one orbit corrector per cell, it must correct for the effects of 8 interconnects that can be averaged in betatron function and phase. The resulting perturbation is of the order of 0.15 mm, *i.e.*, a very modest fraction of the corrector capability.

Tune Shift

The phase advance, $\Delta\mu_{\rm sec}^{\rm i,e}$, produced on the internal (or external) aperture beam by the normal quadrupole field perturbation, $\Delta B_2^{\rm i,e}$, integrated over the ~205 interconnects of a given sector, can be estimated as

$$\Delta\mu_{\rm sec}^{\rm i,e} \approx \frac{205\,\langle\bar{\beta}_{\rm int}\rangle_{\rm cel}}{4\pi} \frac{\int_{\rm int} {\rm d}\sigma\, \Delta B_2^{\rm i,e}(\sigma)}{(B\rho)\,R_{\rm ref}} \qquad (3)$$

where $\langle\bar{\beta}_{\rm int}\rangle_{\rm cel}$ is the average beta function value at the interconnect (80 m). As the beam goes around the ring, it traverses 4 sectors in the internal aperture and 4 sectors in the external aperture, with a change of sign in the main busbar currents. Table 3 gives the maximum phase shift per sector and the maximum tune shift. These values appear significant, but well in the range of correctors.

Coupling Strength

The strength of the linear coupling, $\lvert c_{\rm sec}^{\rm i,e}\rvert$, induced on the internal (resp., external) beam by the skew quadrupole field perturbation, $\Delta A_2^{\rm i,e}$, integrated over the ~205 interconnects of a given sector, can be bounded by

$$\lvert c_{\rm sec}^{\rm i,e}\rvert \le \frac{205\int_{\rm int} {\rm d}\sigma\, \sqrt{\beta_{\rm x}(\sigma)\beta_{\rm y}(\sigma)}\,\Delta A_2^{\rm i,e}(\sigma)}{2\pi\,(B\rho)\,R_{\rm ref}} \qquad (4)$$

where $\sqrt{\beta_{\rm x}(s)\beta_{\rm y}(s)}$ is almost invariant and is taken equal to 80 m. Table 3 shows that, in this simplified analysis where all interconnects add up coherently, the contribution is again small but detectable and is likely to deserve correction.

Linear Chromaticity

The contribution of the sextupole field perturbation to the linear chromaticity appears to be totally negligible.

CONCLUSION

This analysis shows that no significant perturbation to the beam dynamics should be expected due to the parasitic field of the interconnects. Some perturbations are however not negligible and the most realistic and detailed scenario of busbar excitations could be included in the MAD magnetic model of the machine. We also need to check the connection cryostat and DFB effects.

REFERENCES

[1] O. Brüning, P. Collier, *et al.*, LHC Design Report, Vol. 1, CERN 2004-003, 4 June 2004.

[2] S. Russenschuck, *Electromagnetic Design and Mathematical Optimization Methods in Magnet Technology*, at http://cern.ch/russ, 3rd ed., Feb 2006.